Mode Transition and Fault Tolerant Control under Rotor-tilt Axle Stuck Fault of Quad-TRUAV ⋆

Zhong Liu * **Didier Theilliol** ** **Liying Yang** *** **Yuqing He** *** **Jianda Han** ***

* *State Key Laboratory of Robotics, Shenyang Institute of Automation, Chinese Academy of Sciences, 110016, Shenyang, Liaoning Province, P.R.China. University of Chinese Academy of Sciences, 100049, Beijing, P.R.China, (e-mail: liuzhong@sia.cn)*
** *CRAN UMR 7039, CNRS, University of Lorraine, Faculte des Sciences et Techniques, B.P. 70239, 54506 VANDOEUVRE-LES-NANCY, France, (e-mail: didier.theilliol@univ-lorraine.fr)*
*** *State Key Laboratory of Robotics, Shenyang Institute of Automation, Chinese Academy of Sciences, 110016, Shenyang, Liaoning Province, P.R.China, (e-mail: yangliying@sia.cn, heyuqing@sia.cn, and jdhan@sia.cn)*

Abstract: Tilt rotor unmanned aerial vehicle (TRUAV) is a transformable aircraft with abilities of hovering and high-speed cruise. Its transition control is still a difficult point due to varying structure and dynamic behaviour. The main contribution of this paper is to put forward a transition control method based on backstepping for a quad-TRUAV, and fault tolerant control is researched to keep its cruise ability under rotor-tilt axle stuck fault. Explicit mode transition would be avoided by regarding rotor-tilt angle as a control input generated from decoupling with virtual control variables. Numerical results in transition procedure and facing rotor-tilt axle faults are provided to illustrate control effectiveness.

Keywords: Tilt rotor unmanned aerial vehicle, transition procedure, nonlinear control, backstepping, stuck fault, fault tolerant control

1. INTRODUCTION

To break limitations caused by typical structures of conventional unmanned aerial vehicles (UAVs), plentiful hybrid aircraft are researched for wide applications. These aircraft own abilities of hovering and high-speed cruise, so are always accompanied with better flexibility and more endurance than fixed-wing UAVs (FWUAVs) and rotorcraft UAVs (RUAVs), see Saeed et al. (2015). This paper focuses on tilt rotor UAV (TRUAV) that relies on wings and rotors for generating lift together, and is one of hybrid aircraft, see Liu et al. (2017a).

With fixed rotor-tilt angle at $\pi/2$ or 0, the control of TRUAV is similar with conventional RUAV or FWUAV, and regarded in helicopter mode or airplane mode. However, the rotor-tilt angle is not invariable in the transition procedure for acceleration or deceleration. In this procedure, TRUAV is with varying structure and dynamics, which would lead to complex coupling of control effects from rotors and aerodynamic parts. To deal with this problem, gain scheduling (GS) methods are always applied especially in practice, see Muraoka et al. (2012), Zhao et al. (2014), and Liu et al. (2017b). In these methods, rotor-tilt angle plays the role of a flag value representing TRUAV structure, and a set of linear controllers in different angles can be designed for interpolation (Muraoka et al. (2012) and Liu et al. (2017b)) or direct switch (Zhao et al. (2014)) with explicit mode transition. To connect the variation of this flag value with varying dynamics, a special flight envelope called tilt corridor has to be considered in the transition procedure, see Liu et al. (2017b). With this idea, the stability of final flight status in the helicopter mode or airplane mode is focused, but the stability in the transition procedure has not be proved in theory under GS idea.

According to typical tilt corridor in Liu et al. (2017a), different rotor-tilt angles limit different maximum and minimum flight velocities of TRUAV. That means rotor tilt and velocity variation are affected close with each other. As for actual platform, rotor-tilt axle is usually driven by servo through link mechanisms or chains. If it is stuck at one fixed angle, the transition procedure would be broken off, which might be fatal. Fault tolerant control (FTC) methods for aerial vehicles and other systems have been researched for a long time, and many active and passive FTC strategies have been presented, see Qi et al. (2014), Jiang et al. (2012), and Zhang et al. (2008). However, this special stuck fault for TRUAV has not been considered by any existing reference.

⋆ This study was supported by the National Natural Science Foundation of China (Nos. U1608253 and U1508208).

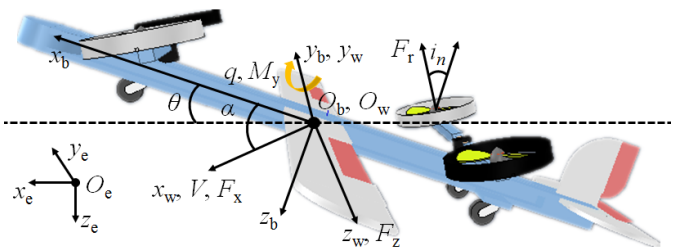

Fig. 1. Quad-TRUAV and coordinate systems

The main contribution of this paper focuses on the design of a hierarchical transition control method for the quad-TRUAV, and a fault tolerant strategy for rotor-tilt axle stuck fault is researched further. In this method, the rotor-tilt angle is regarded as a control input with similar effect as angle of attack. To deal with coupled control inputs and to decouple original dynamics, virtual control variables are considered by backstepping, and decoupling module is applied for control inputs. After rotor-tilt axle stuck fault, a degraded dynamic model is considered, and the decoupling module is also redesigned.

Reminding parts of this paper are organized as follows. Section 2 introduces the longitudinal modeling of quad-TRUAV. Section 3 introduces details of transition controller, including nonlinear controller for virtual control variables and decoupling module for control inputs. Section 4 introduces actuator stuck fault and fault tolerant strategy based on degraded model. Section 5 presents some numerical results to show the control effectiveness. Section 6 ends the whole paper with conclusion.

2. QUAD-TRUAV MODELING

Quad-TRUAV is equipped with two pairs of tiltable rotors that tilt together as shown in Fig. 1. With this structure, the impact caused by the rotor downwash could be alleviated effectively, and would be ignored in TRUAV modeling. The definitions of wind-axis coordinate system ($O_w x_w y_w z_w$), body-axis coordinate system ($O_b x_b y_b z_b$), and north-east-down(NED) coordinate system ($O_e x_e y_e z_e$) are also shown in Fig. 1 according to Cai et al. (2011) and Stengel (2004). Based on these coordinate systems, some states, including flight velocity V, flight height h, angle of attack α, pitch angle θ, and pitch rate q, are defined.

In transition procedure, only longitudinal model is considered. Similar with FWUAVs, dynamics and kinematics equations of TRUAV in wind-axis coordinate system can be formulated as follows according to Stengel (2004):

$$\dot{V} = \frac{F_x}{m}, \tag{1}$$

$$\dot{h} = V\sin(\theta - \alpha), \tag{2}$$

$$\dot{\alpha} = \frac{F_z}{mV} + q, \tag{3}$$

$$\dot{q} = \frac{M_y}{I_y}, \tag{4}$$

$$\dot{\theta} = q, \tag{5}$$

where m is mass, I_y and M_y are rotational inertia and resultant moment in y-direction of body-axis coordinate system, F_x and F_z are resultant forces in x- and z-direction of wind-axis coordinate system. Further considering these forces and moment, F_* is the addition of three components from rotors (F_{*r}), aerodynamic parts (F_{*a}), and gravity (F_{*g}), where $*$ represents x or z for different directions, and resultant moment is the addition of two components from rotors (M_{yr}) and aerodynamic parts (M_{ya}).

Rotors are driven by brushless direct current motors. Generated forces are proportional to the square of rotor speeds, see Pounds et al. (2010). Further transform them into wind-axis coordinate system, following component forces and moment are obtained:

$$F_{xr} = 2C_t\rho AR^2\cos(\alpha + i_n)(\Omega_f^2 + \Omega_b^2), \tag{6}$$

$$F_{zr} = -2C_t\rho AR^2\sin(\alpha + i_n)(\Omega_f^2 + \Omega_b^2), \tag{7}$$

$$M_{yr} = 2C_t\rho AR^2 x_r \sin i_n(\Omega_f^2 - \Omega_b^2), \tag{8}$$

where i_n represents rotor-tilt angle, C_t is tension coefficient, ρ is air density, A is rotor area, R is rotor radius, Ω_f and Ω_b are forward and backward rotor speeds, and x_r is longitudinal distance from center of gravity to rotors.

As for aerodynamic forces and moment, all aerodynamic parts can be transformed into the same size by scaling aerodynamic coefficients. According to Zhao et al. (2014), following aerodynamic forces and moment are obtained:

$$F_{xa} = 1/2\rho V^2 S \cdot C_D = 1/2\rho V^2 S \cdot C_{D0}, \tag{9}$$

$$F_{za} = 1/2\rho V^2 S \cdot C_L = 1/2\rho V^2 S \cdot (C_{L0} + C_{L\alpha}\alpha), \tag{10}$$

$$M_{ya} = 1/2\rho V^2 S\bar{c} \cdot C_M = 1/2\rho V^2 S\bar{c} \cdot (C_{M0} + C_{M\delta}\delta_e), \tag{11}$$

where S and $\bar{c}$ are the equivalent wing area and mean chord length, C_D, C_L, and C_M are aerodynamic coefficients, and subscripts D, L, and M mean drag, lift, and pitch moment. In these coefficients, some items are disregarded for simplifications of nonlinear modeling and controller design. δ_e is deflection of elevator.

Considering gravity further, following component forces are formed:

$$F_{xg} = -mg\sin(\theta - \alpha), \tag{12}$$

$$F_{zg} = mg\cos(\theta - \alpha), \tag{13}$$

where g is gravitational acceleration.

Introducing forces and moments (6)$\sim$(13) into (1)$\sim$(5), mathematical model of quad-TRUAV can be formulated as a typical nonlinear system as follows:

$$\dot{x}(t) = f(x(t), u_o(t)), \tag{14}$$

$$y(t) = h(x(t)) \triangleq Ix(t), \tag{15}$$

where $x(t) = [V\ h\ \gamma\ \alpha\ q]^T$ is state vector, $\gamma = \theta - \alpha$ is defined as track angle, $u_o(t) = [i_n\ \Omega_f\ \Omega_b\ \delta_e]^T$ is control input vector, $y(t)$ is output vector, and I is an unit matrix to assume all states are measurable.

Note that, regarding i_n as a control input in this paper, explicit mode transition in conventional GS method could be avoided. And this value is no necessarily limited in $[0, \pi/2]$ for necessary control effect. More details of TRUAV modeling and parameters could refer to Pounds et al. (2010) and Zhao et al. (2014).

3. TRACKING CONTROL SYNTHESIS

Based on a dynamic decoupling approach, the structure of tracking controller for transition procedure would be formulated firstly in this section. According to this structure, details of nonlinear controller and decoupling design would be introduced mainly.

3.1 Decoupling-based Controller Formulation

With generalized representations in (14) and (15), every state in $x(t)$ can be regarded as a degree-of-freedom (DoF). Because of under-actuated characteristics and varying structure, some DoFs of TRUAV are coupled and with complex coupling of control inputs. It is obviously shown in (6)∼(8) and (11) with i_n as one control input. To avoid considering this coupling in controller design directly, virtual control variables are defined as follows:

$$v_1(t) \triangleq F_V - g\sin\gamma,$$
$$v_2(t) = \begin{bmatrix} v_{21}(t) \\ v_{22}(t) \end{bmatrix} \triangleq \begin{bmatrix} F_\alpha - \frac{\rho S}{2m} C_{\mathrm{L}\alpha} V \alpha \\ M_q \end{bmatrix},$$

where intermediate variables

$$F_V = \frac{2\rho A R^2}{m} C_{\mathrm{t}} \cos(\alpha + i_n)(\Omega_{\mathrm{f}}^2 + \Omega_{\mathrm{b}}^2), \tag{16}$$

$$F_\alpha = -\frac{2\rho A R^2}{mV} C_{\mathrm{t}} \sin(\alpha + i_n)(\Omega_{\mathrm{f}}^2 + \Omega_{\mathrm{b}}^2), \tag{17}$$

$$M_q = \frac{2\rho A R^2 x_{\mathrm{r}}}{I_{\mathrm{y}}} C_{\mathrm{t}} \sin i_n (\Omega_{\mathrm{f}}^2 - \Omega_{\mathrm{b}}^2) + \frac{\rho S \overline{c}}{2I_{\mathrm{y}}} \cdot V^2 C_{\mathrm{M}\delta} \delta_{\mathrm{e}} \tag{18}$$

include all coupled control inputs.

With above definitions, nominal quad-TRUAV model can be reformed with a simple form as follows:

$$\dot{V} = -\frac{\rho S}{2m} C_{\mathrm{D}0} V^2 + v_1(t),$$
$$\dot{h} = V\sin\gamma,\ \dot{\gamma} = \frac{\rho S}{2m} C_{\mathrm{L}0} V - \frac{g\cos\gamma}{V} - v_{21}(t),$$
$$\dot{\alpha} = -\frac{\rho S}{2m} C_{\mathrm{L}0} V + \frac{g\cos\gamma}{V} + v_{21}(t) + q,$$
$$\dot{q} = \frac{\rho S \overline{c}}{2I_{\mathrm{y}}} C_{\mathrm{M}0} V^2 + v_{22}(t).$$

For further controller design, above equations are formulated generally as follows:

$$\dot{x}_1(t) = f_1(x_1(t), v_1(t)), \tag{19}$$
$$\dot{x}_2(t) = f_2(x_1(t), x_2(t), v_2(t)), \tag{20}$$

where $x(t)$ is divided into 2 parts: $x_1(t) = V$ and $x_2(t) = [h\ \gamma\ \alpha\ q]^{\mathrm{T}}$, output vectors $y_1(t) = x_1(t)$ and $y_2(t) = x_2(t)$.

Note that, coupled items about states and control inputs are considered in virtual control variables. (19) and (20) decouple original quad-TRUAV model into several subsystems corresponding to $x_1(1)$ and $x_2(t)$, in which subsystems corresponding to $[h\ \gamma]^{\mathrm{T}}$ and $[\alpha\ q]^{\mathrm{T}}$ are also relatively independent. In this way, nonlinear controllers could be designed for virtual control variables, and control coupling does not need to be considered in nonlinear controllers design. Then, with the forms of intermediate variables (16)∼(18), decoupling module for control inputs can be designed. The structure of transition controller is summarized in Fig. 2, where subscript re represents reference value. The purpose of this controller is to ensure stability and reference tracking in transition procedure

$$\lim_{t\to+\infty} (C_{\mathrm{re}} y(t) - r(t)) = 0,$$

where $r(t)$ is reference vector $[V_{\mathrm{re}}\ h_{\mathrm{re}}\ \alpha_{\mathrm{re}}]^{\mathrm{T}}$, and matrix

$$C_{\mathrm{re}} = \begin{bmatrix} 1 & 0 & 0 & 0 & 0 \\ 0 & 1 & 0 & 0 & 0 \\ 0 & 0 & 0 & 1 & 0 \end{bmatrix}$$

directly because of the unit output matrix in (15).

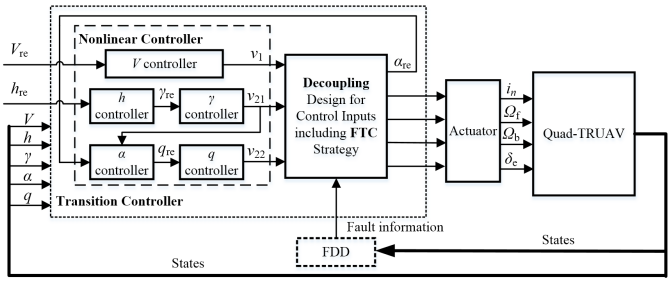

Fig. 2. Transition controller structure

3.2 Nonlinear Controller Design

As analyzed in above subsection, quad-TRUAV model has been transformed into generally nonlinear form (19) and (20) with virtual control variables $v_1(t)$ and $v_2(t)$. So many nonlinear feedback control methods could be applied here for stability and reference tracking.

Considering (19) with unit output matrix in (15), it is a single-input-single-output system. Feedback linearization can be applied directly to formulate following closed-loop system (Khalil (2012)):

$$\dot{x}_1(t) = -k_1(x_1(t) - x_{1\mathrm{re}}(t)) + \dot{x}_{1\mathrm{re}}(t), \tag{21}$$

where k_1 is a positive constant, and $x_{1\mathrm{re}}(t)$ is the reference value. To track reference velocity V_{re} in TRUAV transition procedure, following virtual control variable is obtained:

$$v_1(t) = -k_V(V - V_{\mathrm{re}}) + \dot{V}_{\mathrm{re}} + \frac{\rho S}{2m} C_{\mathrm{D}0} V^2, \tag{22}$$

where k_V is a positive parameter. Intermediate variable F_V in $v_1(t)$ could also be obtained for next subsection.

Further considering (20), this subsystem can be reformulated as follows:

$$\dot{x}_{21}(t) = f_{21}(x_1(t), \dot{x}_{22}(t)) + g_{21}(x_{22}(t)), \tag{23}$$
$$\dot{x}_{22}(t) = f_{22}(x_1(t), x_{22}(t)) + g_{22}(v_2(t)), \tag{24}$$

where $x_{21}(t) = [h\ \alpha]^{\mathrm{T}}$ and $x_{22}(t) = [\gamma\ q]^{\mathrm{T}}$. Considering $\dot{x}_{22}(t)$ in (23) due to $\dot{\alpha} = -\dot{\gamma} + q$, subsystems corresponding to $[h\ \gamma]^{\mathrm{T}}$ and $[\alpha\ q]^{\mathrm{T}}$ could be analyzed separately as shown in Fig. 2. (23) and (24) are with strict feedback form, and this form is caused by inherently under-actuated characteristics of UAV. In this way, a hierarchical controller from bacskstepping would be a good choice, see Khalil (2012) and Loza et al. (2015). Concretely speaking, for (23), assume there is a Lypunov function $\mathcal{V}_{21}(x_{21}(t))$ satisfies stability conditions with $x_{22}(t) = x_{22\mathrm{re}}(t)$, which means

$$\mathcal{V}_{21}(x_{21}(t)) > 0, \text{ and } \dot{\mathcal{V}}_{21}(x_{21}(t))|_{x_{22}=x_{22\mathrm{re}}} < 0$$

with nonzero state vector $x_{21}(t)$. Further define $e_{22}(t) = x_{22}(t) - x_{22\mathrm{re}}(t)$ and alternative Lyapnov function

$$\mathcal{V}_2(x_{21}(t), e_{22}(t)) = \mathcal{V}_{21}(x_{21}(t)) + \frac{1}{2} e_{22}^{\mathrm{T}}(t) e_{22}(t).$$

Obviously,

$$\begin{aligned} \dot{\mathcal{V}}(x_{21}(t), e_{22}(t)) =& \dot{\mathcal{V}}_{21}(x_{21}(t))|_{x_{22}=x_{22\mathrm{re}}} + (\dot{\mathcal{V}}_{21}(x_{21}(t)) \\ & - \dot{\mathcal{V}}_{21}(x_{21}(t))|_{x_{22}=x_{22\mathrm{re}}}) + (x_{22}(t) \\ & - x_{22\mathrm{re}}(t))^{\mathrm{T}}(\dot{x}_{22}(t) - \dot{x}_{22\mathrm{re}}(t)). \end{aligned}$$

If $v_2(t)$ is constructed and ensures

$$\begin{aligned} &(\dot{\mathcal{V}}_{21}(x_{21}(t)) - \dot{\mathcal{V}}_{21}(x_{21}(t))|_{x_{22}=x_{22\mathrm{re}}}) \\ &+ (x_{22}(t) - x_{22\mathrm{re}}(t))^{\mathrm{T}}(\dot{x}_{22}(t) - \dot{x}_{22\mathrm{re}}(t)) < 0, \end{aligned}$$

the stability of $x_2(t)$ can be obtained eventually.

With above idea, for tracking reference flight height $h_{\rm re}$ and reference angle of attack $\alpha_{\rm re}$, following virtual control variables are obtained:

$$\begin{aligned} v_{21}(t) =& k_\gamma(\gamma-\gamma_{\rm re})-\dot\gamma_{\rm re}+\frac{\rho S}{2m}C_{\rm L0}V-\frac{g\cos\gamma}{V} \\ &+(h-h_{\rm re})V\frac{\sin\gamma-\sin\gamma_{\rm re}}{\gamma-\gamma_{\rm re}}, \end{aligned} \tag{25}$$

$$v_{22}(t)=-k_q(q-q_{\rm re})+\dot q_{\rm re}-\frac{\rho S\bar c}{2I_{\rm y}}C_{\rm M0}V^2-(\alpha-\alpha_{\rm re}), \tag{26}$$

where

$$\gamma_{\rm re}=-{\rm sign}(V(h-h_{\rm re}))\frac{|h-h_{\rm re}|}{H}\pi, \tag{27}$$

$$\begin{aligned} q_{\rm re}=&-k_\alpha(\alpha-\alpha_{\rm re})+\dot\alpha_{\rm re}-k_\gamma(\gamma-\gamma_{\rm re})+\dot\gamma_{\rm re} \\ &-(h-h_{\rm re})V\frac{\sin\gamma-\sin\gamma_{\rm re}}{\gamma-\gamma_{\rm re}}, \end{aligned} \tag{28}$$

H, k_γ, k_α, and k_q are all positive parameters, and ${\rm sign}(\cdot)$ represents sign calculation. Intermediate variables F_α and M_q in $v_2(t)$ could also be obtained for decoupling design.

The detailed stability analysis can be seen in Appendix A.

3.3 Decoupling Design for Control Inputs

There is no doubt that coupled items in original model would not "decrease" or "increase". Now that original model is decoupled by virtual control variables, that means serious coupling is included in $v_1(t)$ and $v_2(t)$. In controller design based on decoupled dynamics, a decoupling module with inputs as virtual control variables and outputs as control inputs should be designed, see Nordfeldt et al. (2006). However, decoupling designs are absolutely different facing different controlled plants, and dependent on actuator dynamics that could be represented as following generalized form (Ahmed et al. (2010)):

$$\begin{bmatrix} v_1(t)\\ v_2(t)\end{bmatrix}=\begin{bmatrix} m_1(x_1(t),x_2(t),u_{\rm o}(t))\\ m_2(x_1(t),x_2(t),u_{\rm o}(t))\end{bmatrix}. \tag{29}$$

With above equation, decoupling modules are inverse functions of $m_1(\cdot)$ and $m_2(\cdot)$ for unknown vector $u_{\rm o}(t)$.

Note that, actuator fault has not been introduced here, so outputs of decoupling module are control inputs $u_{\rm o}(t)$ exactly, as shown in (29). However, in faulty case, outputs should be rewritten as inputs of actuator module, as shown in Fig. 2. Decoupling design for quad-TRUAV is not more than a algebraic problem. Algebraic forms of intermediate variables (16)$\sim$(18) would be analyzed mainly for control inputs, because they include all coupled control inputs.

According to (16) and (17), $\alpha+i_n=\arctan(-\frac{VF_\alpha}{F_V})$. In transition procedure, i_n could compensate the control effect of angle of attack as follows:

$$i_n=\arctan(-\frac{VF_\alpha}{F_V})-\alpha. \tag{30}$$

The reference value of α can be set according to target value of rotor tilt angle as follows:

$$\alpha_{\rm re}=\begin{cases} \alpha_\tau, & i_n>0\\ \dfrac{1}{T_\alpha s+1}\arctan(-\dfrac{VF_\alpha}{F_V}), & i_n\le 0\end{cases}, \tag{31}$$

where α_τ is a constant reference, and T_α is a time constant of the low-pass filter, which is used to remove underlying algebraic loop in case that $\alpha_{\rm re}$ depends on α directly. For normal transition procedure, α_τ can be set according to required acceleration. Obviously, with (30) and (31), quad-TRUAV can be stabilized at rotor-tilt angle 0, and i_n takes the whole control effect in transition procedure until it reaches given target value 0. With application of low-pass filter in (31), i_n would less than 0 momentarily to compensate control effect in the end of transition procedure because of the delayed response of α to $\arctan(-\frac{VF_\alpha}{F_V})$.

For other control inputs, $\Omega_{\rm f}^2+\Omega_{\rm b}^2$ are included in (16) and (17). So

$$\Omega_{\rm f}^2+\Omega_{\rm b}^2=\frac{m\sqrt{F_V^2+(VF_\alpha)^2}}{2\rho AR^2C_{\rm t}}. \tag{32}$$

As shown in (18), rotors and elevator are all included in M_q, and could take control effect concurrently in transition procedure. To deal with this redundancy, define rotor control weight η firstly. With the form of M_q and $\eta\in[0,1]$,

$$\Omega_{\rm f}^2-\Omega_{\rm b}^2=\frac{\eta M_q}{\frac{2\rho AR^2x_{\rm r}}{I_{\rm y}}C_{\rm t}\sin i_n}, \tag{33}$$

$$\delta_{\rm e}=\frac{(1-\eta)M_q}{\frac{\rho S\bar c}{2I_{\rm y}}\cdot V^2C_{\rm M\delta}}. \tag{34}$$

η should represent the weight of control effect from rotors according to TRUAV structure or flight velocity. Similar weight value is also applied in GS method, but there is not a theoretical form of this value. For decoupling here,

$$\eta=1-\frac{V^2}{V_{\rm c}^2},$$

where $V_{\rm c}$ is the regular cruise speed in airplane mode.

In general, control inputs i_n, $\Omega_{\rm f}$, $\Omega_{\rm b}$, and $\delta_{\rm e}$ are obtained by (30) and (32)$\sim$(34). Note that, if $\Omega_{\rm f}^2+\Omega_{\rm b}^2<\Omega_{\rm f}^2-\Omega_{\rm b}^2$, that would cause $\Omega_{\rm b}^2<0$, which is unpractical. To ensure $\Omega_{\rm f}^2\ge 0$ and $\Omega_{\rm b}^2\ge 0$, reasonable planning for $V_{\rm re}$ and $h_{\rm re}$ is necessary, and low-pass filter in (31) is also helpful.

4. FAULT TOLERANT DESIGN

4.1 Actuator Stuck Fault

According to Qi et al. (2016), actuator stuck fault can be defined as follows:

$$u_{\rm o}(t)=\Phi(t)u_{\rm i}(t)+(I-\Phi(t))u_{\rm F}.$$

Above equation corresponds to actuator module in Fig. 2, where $u_{\rm o}(t)$ represents control inputs of controlled plant in (14) and actuator outputs, $u_{\rm i}(t)$ is actuator inputs, and $u_{\rm F}$ is a constant vector representing the magnitude of stuck failure. $\Phi(t)={\rm diag}(\phi_1(t),...,\phi_i(t),...,\phi_m(t))$, $\phi_i(t)=1$ means ith actuator is fault-free, and $\phi_i(t)=0$ represents ith actuator is faulty and lock-in-place.

For following FTC strategy, assume fault information can be estimated accurately and timely by fault detection and diagnosis (FDD) module. Because there are lots of mature methods can be applied here, see Blanke et al. (2006) and Qi et al. (2012), FDD for matrix Φ and vector $u_{\rm F}$ of actuator fault is not considered further in this paper.

4.2 Degraded Model Approach

Different with TRUAV control at any rotor-tilt angle, the rotor-tilt axle could not respond to actuator input after

stuck fault, and faulty model can be formulated as (19) and (20) with $v_1(t)$ and $v_2(t)$ replaced by

$$v_{1_{\mathcal{F}}}(t) \triangleq m_1(x_1(t), x_2(t), u_{\rm o}(t)|_{i_n=i_{n_{\mathcal{F}}}}), \text{ and}$$
$$v_{2_{\mathcal{F}}}(t) \triangleq m_2(x_1(t), x_2(t), u_{\rm o}(t)|_{i_n=i_{n_{\mathcal{F}}}}),$$

where subscript $\mathcal{F}$ means equation with fault, and $i_{n_{\mathcal{F}}}$ represents faulty rotor-tilt angle. In this case, a control input is lost. A degraded model can be used to ensure partial control performance, see Souanef et al. (2015).

To obtain this degraded model, dynamics of controlled plant should be analyzed: similar with fixed-wing aircraft, TRUAV would not be accompanied with diverging states with stable flight height and angle of attack (Stengel (2004)), so angle of attack control and flight height control are much more important for safe flight. That means only

$$\dot{x}_2(t) = f_2(x_1(t), x_2(t), v_{2_{\mathcal{F}}}(t)) \tag{35}$$

needs to be kept as degraded model, and $x_1(t)$ is in a open loop as follows:

$$\dot{x}_1(t) = f_1(x_1(t), v_{1_{\mathcal{F}}}(t))$$

compared with closed-loop form in fault free case (21).

Assume $i_{n_{\mathcal{F}}}$ can be measured or estimated by FDD module after a small delay. With above idea, discarding tracking control of flight velocity, virtual control variable $v_{2_{\mathcal{F}}}(t)$ could still be obtained from (25)$\sim$(28) to track references of flight height and angle of attack, and re-decoupled control inputs are constructed as follows and (34):

$$\alpha_{\rm re} = \alpha_{{\rm re}_{\mathcal{F}}},$$
$$\Omega_{\rm f}^2 + \Omega_{\rm b}^2 = \frac{F_\alpha}{-\frac{2\rho A R^2}{mV} C_{\rm t} \sin(\alpha + i_{n_{\mathcal{F}}})},$$
$$\Omega_{\rm f}^2 - \Omega_{\rm b}^2 = \frac{\eta M_q}{\frac{2\rho A R^2 x_{\rm r}}{I_{\rm y}} C_{\rm t} \sin i_{n_{\mathcal{F}}}},$$

where $\alpha_{{\rm re}_{\mathcal{F}}}$ is a adjustable reference value for angle of attack after stuck fault.

With reconstructed decoupling, height tracking is still feasible, and angle of attack is stabilized at $\alpha_{{\rm re}_{\mathcal{F}}}$. According to quad-TRUAV dynamics model, flight velocity would research a new stabilized value when $t \to +\infty$ as follows:

$$V_\infty \triangleq \lim_{t\to+\infty} V(t) = -\frac{2mF_{\alpha\infty}}{\rho S C_{\rm D0} \tan(\alpha_{{\rm re}_{\mathcal{F}}} + i_{n_{\mathcal{F}}})}$$
$$= \sqrt{\frac{2mg}{\rho S(C_{\rm L0} + C_{\rm L\alpha}\alpha_{{\rm re}_{\mathcal{F}}} + C_{\rm D0}\tan(\alpha_{{\rm re}_{\mathcal{F}}} + i_{n_{\mathcal{F}}}))}}, \tag{36}$$

where $F_{\alpha\infty} \triangleq \lim_{t\to+\infty} F_\alpha$ is the stabilized value of F_α.

Note that, according to (36), new stabilized velocity V_∞ is determined by given reference value of angle of attack $\alpha_{{\rm re}_{\mathcal{F}}}$. This provides some control freedom of velocity facing rotor-tilt axle stuck fault, and V_∞ can be regarded as a redesigned reference value. V_∞ is always researchable with suitable $\alpha_{{\rm re}_{\mathcal{F}}}$, and actuator saturation is not easy to meet due to degraded model approach. However, the rang of angle of attack should be paid attention in case of stall.

5. NUMERICAL RESULTS

For following numerical results, model parameters in Section 2 are listed as $m = 2.71$, $I_{\rm y} = 0.0816$, $\bar{c} = 0.2966$,

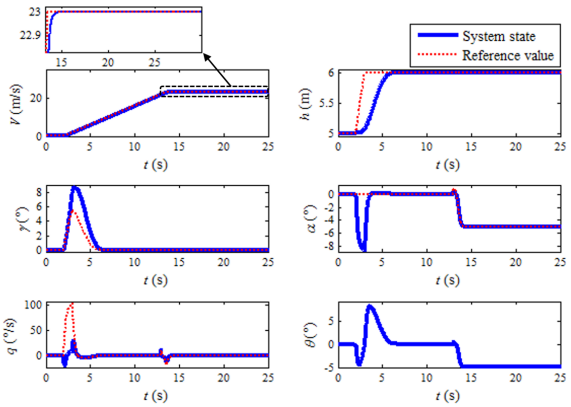

Fig. 3. Curves of states in transition procedure

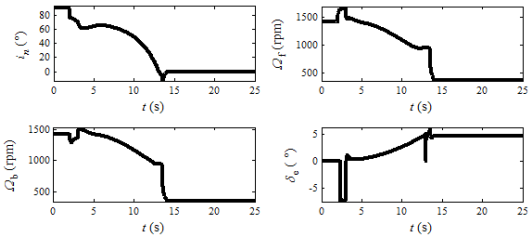

Fig. 4. Curves of control inputs

$S = 0.453$, $R = 0.12$, $A = R^2\pi$, $x_{\rm r} = 0.1847$, $C_{\rm t} = 0.0041$, $C_{\rm D0} = 0.0111$, $C_{\rm L0} = 0.1982$, $C_{\rm M0} = 0.0189$, and $C_{\rm M\delta} = -0.23728$. Furthermore, controller parameters in Section 3 are listed as $k_V = 5$, $H = 30$, $k_\gamma = 30$, $k_\alpha = 10$, $k_q = 8$, $T_\alpha = 1$, and $V_{\rm c} = 21$.

5.1 Results of Fault-free Transition Procedure

Set the initial values of V and h as 0.001 and 5, and their final reference values as 23 and 6. Curves of states and control inputs are shown in Fig. 3 and Fig. 4.

In the beginning of numerical simulation, quad-TRUAV is with 90° rotor-tilt angle, and this value is reduced for acceleration after 2s. Then, α is stabilized at α_τ ($\alpha_\tau = 0$ here), and i_n takes main control effect. When i_n reaches 0, TRUAV should be set in airplane mode, and $\alpha_{\rm re}$ should be with varying value according to (31). Because of the delayed response of α, rotor-tilt angle researches negative value for compensation, and stabilized at 0 in the end that means transition from helicopter mode to airplane mode is realized. For actual servo actuators, negative rotor-tilt angle is realizable. The flight height is also kept in whole transition procedure. Above numerical results represent the effectiveness of transition controller in Section 3.

Curve of rotor control weight is shown in Fig. 5. With this weight value, to ensure $\Omega_{\rm f}^2 \geq 0$ and $\Omega_{\rm b}^2 \geq 0$, continuous step signals are applied for velocity and height references with fixed slops as $2{\rm m/s}^2$ and $1{\rm m/s}$, which could also slow down the descending rate of rotor-tilt angle.

5.2 Results under Rotor-tilt Axle Stuck Fault

Assume the stuck fault at 30° as a sample, and this faulty value can be measured or estimated 0.2s later, which can be regarded as FDD delay. Set the initial values of V

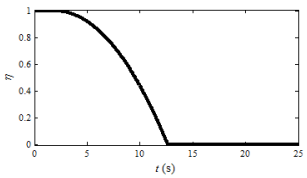

Fig. 5. Curve of controller weight

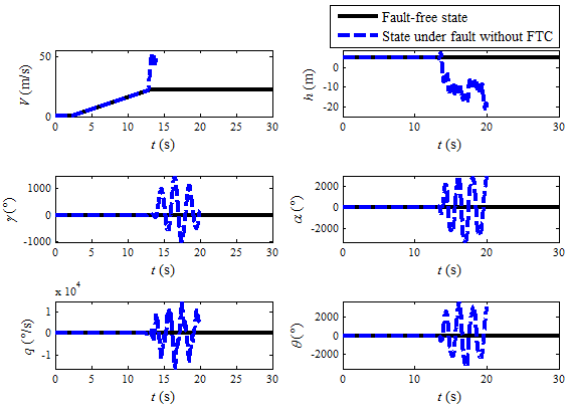

Fig. 6. Curves of states without FTC compared with fault-free states

and h at 0.001 and 5 also, and their final references are set as 22 and 5 with fixed slopes as 2m/s^2 and 1m/s. Curves of states without and with FTC strategy compared with fault-free states are shown in Fig. 6 and Fig. 7, and curves of rotor-tilt angle are shown in Fig. 8. After stuck fault, common transition controller would still regard i_n as a control input, and keep tracking velocity reference. This would lead to instability as shown in Fig. 6. With FTC strategy introduced in Section 3 and $\alpha_{\text{re}_\mathcal{F}} = 0$, flight height can still track reference value, and angle of attack is stabilized at $\alpha_{\text{re}_\mathcal{F}}$ as shown in Fig. 7. According to (36), flight velocity would not track reference value 22m/s, and be stabilized at 21.66m/s when $t \to +\infty$. Above numerical results show that proposed FTC strategy can ensure safe status after stuck fault, and keep the cruise ability with fixed rotor-tilt angle.

Further consider the value of $\alpha_{\text{re}_\mathcal{F}}$. If faster or lower flight velocity is needed, $\alpha_{\text{re}_\mathcal{F}}$ can be set as a negative or positive value according to (36). As shown in Fig. 9, setting $\alpha_{\text{re}_\mathcal{F}}$ as $-10°$, 0, and $10°$ with $70°$ rotor-tilt axle stuck fault, redesigned velocity references 22.27m/s, 20.49m/s, and 18.1m/s can be obtained, and actual velocity would be stabilized at them in the end, respectively. Although rate of convergence is slow, quad-TRUAV is still with the ability of tracking velocity reference in a degree by $\alpha_{\text{re}_\mathcal{F}}$. However, the permissible range of angle of attack should be taken into consideration.

Above numerical results are all with 0.2s FDD delay. To test the effect of FDD delay for FTC, following performance criteria are defined:

$$e_1 = \int_0^{t_e} (C_{\text{re}}x(t) - r(t))^{\text{T}} Q (C_{\text{re}}x(t) - r(t))\text{dt},$$

$$e_2 = \int_0^{t_e} u_{\text{o}}(t)^{\text{T}} R u_{\text{o}}(t)\text{dt},$$

where t_e is simulation time, Q and R are all weight matrices with diagonal forms. After stuck fault, V_{re} in $r(t)$

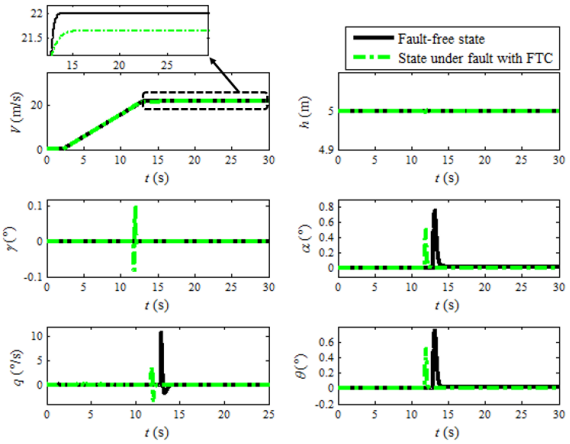

Fig. 7. Curves of states with FTC compared with fault-free states

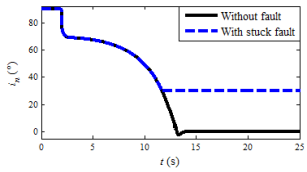

Fig. 8. Curve of rotor-tilt angle with 30° stuck fault

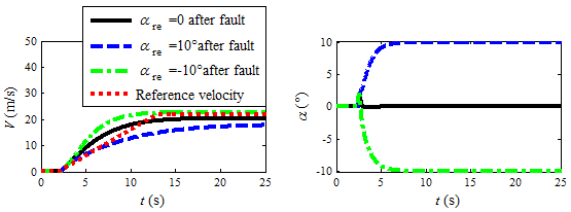

Fig. 9. Curves of V and α with different α_{re} after 70° rotor-tilt axle stuck fault

Table 1. Criteria with different FDD delays

FDD delay (s)	0.1	0.2	0.3	0.33	0.34
Criterion e_1	13.87	15.98	18.56	31.97	$+\infty$
Criterion e_2	723224	723248	723271	723413	$+\infty$

would be replaced by V_∞. So e_1 represents tracking performance, and e_2 represents consumed energy. With 45° stuck fault, same initial values and reference values with above example, $\alpha_{\text{re}_\mathcal{F}} = 0$, and $t_e = 100$, $Q = \text{diag}(1, 10^6, 10^5)$, $R = \text{diag}(10, 0.01, 0.01, 10^5)$, criteria with different FDD delays are listed in Table 1. According to this table, larger FDD delay leads to worse tracking performance and more energy consumption, and might result in instability in spite of FTC. That means proposed FTC strategy requires real-time performance of FDD methods.

6. CONCLUSION

In conclusion, this paper proposes a new idea of transition controller for quad-TRUAV. Different with GS methods, rotor-tilt angle is regarded as a control input, and virtual control variable including more than one control inputs is considered to decouple original dynamics. In this way, explicit mode transition is avoided. Hierarchical nonlinear controller based on backstepping and decoupling module are designed for virtual control variables and control

inputs, respectively. Moreover, rotor-tilt axle stuck fault is considered further. By reconstructing decoupling module, FTC strategy could ensure the cruise ability by setting a fixed angle of attack reference, and keep flight height tracking. Comparing defined performance criteria, real-time FDD methods are required for above FTC strategy.

REFERENCES

Saeed, A., Younes, A., Islam, S., Dias, J., Seneviratne, L., and Cai, G. (2015). A review on the platform design, dynamic modeling and control of hybrid UAVs. 2015 International Conference on Unmanned Aircraft Systems (ICUAS), Denver, Colorado, USA, Jun. 9-12, 2015.

Liu, Z., He, Y., Yang, L., and Han, J. (2017a). Control techniques of tilt rotor unmanned aerial vehicle systems: A review. *Chinese Journal of Aeronautics*, 30(1), 135-148.

Muraoka, J., Okada, N., Kubo, D., and Sato, M. (2012). Transition flight of quad tilt wing VTOL UAV. 28th congress of the international council of the aeronautical sciences (ICAS), 2012.

Zhao, W., and Underwood, C. (2014). Robust transition control of a Martian coaxial tiltrotor aerobot. *Acta Astronautica*, 99, 111-129.

Liu, Z., Theilliol, D., Yang, L., He, Y., and Han, J. (2017b). Transition control of tilt rotor unmanned aerial vehicle based on multi-model adaptive method. 2017 International Conference on Unmanned Aircraft Systems (ICUAS), Miami, Florida, USA, Jun. 13-16, 2017.

Qi, X., Qi, J., Theilliol, D., Zhang, Y., Han, J., Song, D., and Hua, C. (2014). A review on fault diagnosis and fault tolerant control methods for single-rotor aerial vehicles. *Journal of Intelligent & Robotic Systems*, 73, 535-555.

Jiang, J., and Yu, X. (2012). Fault-tolerant control systems: A comparative study between active and passive approaches. *Annual Reviews in Control*, 36, 60-72.

Zhang, Y., and Jiang, J. (2008). Bibliographical review on reconfigurable fault-tolerant control systems. *Annual Reviews in Control*, 32, 229-252.

Cai, G., Chen, B., and Lee, T. (2011). *Unmanned rotorcraft system*, 23-34. Springer, Germany.

Stengel, R. (2004). *Flight dynamics*, 29-146, 451-572. Princeton University Press, Oxfordshire, UK.

Pounds, P., Mahony, R., and Corke, P. (2010). Modelling and control of a large quadrotor robot. *Control Engineering Practice*, 18, 691-699.

Khalil, H. (2012). *Nonlinear systems, third edition*, 505-550, 589-603. Publishing House of Electronics Industry, Beijing, P.R.China.

Loza, A., Henry, D., Zolghadri, A., and Fridman, L. (2015) Output tracking of systems subjected to perturbations and a class of actuator faults based on HOSM observation and identification. *Automatic*, 59, 200-205.

Nordfeldt, P., and Hagglund, T. (2013). Decoupler and PID controller design of TITO systems. *Journal of Process Control*, 16, 923C936.

Ahmed, B., and Kendoul, F. (2010). Flight control of a small helicopter in unknown wind conditions. 2010 IEEE Conference on Decision and Control (CDC), Atlanta, GA, USA, Dec. 15-17, 2010.

Qi, X., Theilliol, D., Qi, J., Zhang, Y, and Han, J. (2016). Self-healing control against cctuator stuck failures under constraints: application to unmanned helicopters. *Springer International Publishing*, 386, 193-207.

Blanke, M., Kinnaert, M., Lunze, J., and Staroswiecki, M. (2006). *Diagnosis and fault-tolerant control, second edition*, 189-298. Springer, Heidelberg, Berlin.

Qi, J., Song, D., Wu, C., Han, J, and Wang, T. (2012). KF-based adaptive UKF algorithm and its application for rotorcraft UAV actuator failure estimation. *International Journal of Advanced Robotic Systems*, 9, 1-9.

Souanef, T., and Fichter, W. (2015). Fault tolerant L_1 adaptive control based on degraded models. *Advances in Aerospace Guidance, Navigation and Control*, 135-149.

Appendix A. STABILITY PROOF OF NONLINEAR CONTROLLER

As for V, with virtual control variable (22), the closed-loop system can be formed as follows:

$$\dot{V} - \dot{V}_{\rm re} = -k_V(V - V_{\rm re}).$$

With Lyapunov function $\mathcal{V}_V(V - V_{\rm re}) = \frac{1}{2}(V - V_{\rm re})^2$, its derivative

$$\dot{\mathcal{V}}_V(V - V_{\rm re}) = -k_V(V - V_{\rm re})^2 \leq 0.$$

When $t \to +\infty$, V would be asymptotically stable at $V_{\rm re}$.

As for h, with state γ and its reference value (27), Lyapunov function can be chosen as $\mathcal{V}_h(h - h_{\rm re}) = \frac{1}{2}(h - h_{\rm re})^2$, and assume $\gamma \in [-\pi, \pi]$. In this way,

$$\begin{aligned}\dot{\mathcal{V}}_h(h - h_{\rm re}) &= (h - h_{\rm re})\dot{h}|_{\gamma=\gamma_{\rm re}} \\ &= -|V(h - h_{\rm re})|\sin(\frac{|h - h_{\rm re}|}{H}\pi) \leq 0.\end{aligned}$$

h could track constant reference value when $t \to +\infty$, and parameter H can limit the maximum value of $h_{\rm re}$. As for α, state q can be set as

$$q_{\rm re} = -k_\alpha(\alpha - \alpha_{\rm re}) + \dot{\alpha}_{\rm re} + \frac{\rho S}{2m}C_{\rm L0}V - \frac{g\cos\gamma}{V} - v_{21}(t).$$

With Lyapunov function $\mathcal{V}_\alpha(\alpha - \alpha_{\rm re}) = \frac{1}{2}(\alpha - \alpha_{\rm re})^2$, the stability of α can be proven.

Based on the idea of backstepping, further define $e_\gamma = \gamma - \gamma_{\rm re}$ and $e_q = q - q_{\rm re}$, consider Lyapunov functions $\mathcal{V}_\gamma(h - h_{\rm re}, e_\gamma) = \mathcal{V}_h(h - h_{\rm re}) + \frac{1}{2}e_\gamma^2$ and $\mathcal{V}_q(\alpha - \alpha_{\rm re}, e_q) = \mathcal{V}_\alpha(\alpha - \alpha_{\rm re}) + \frac{1}{2}e_q^2$. Their derivatives

$$\begin{aligned}\dot{\mathcal{V}}_\gamma(h - h_{\rm re}, e_\gamma) =&(h - h_{\rm re})V\sin\gamma_{\rm re} + (h - h_{\rm re})V(\sin\gamma \\ &- \sin\gamma_{\rm re}) + (\gamma - \gamma_{\rm re})(\dot{\gamma} - \dot{\gamma}_{\rm re}).\end{aligned}$$

$$\begin{aligned}\dot{\mathcal{V}}_q(\alpha - \alpha_{\rm re}, e_q) =& -k_\alpha(\alpha - \alpha_{\rm re})^2 + (\alpha - \alpha_{\rm re})(q - q_{\rm re}) \\ &+ (q - q_{\rm re})(\dot{q} - \dot{q}_{\rm re}).\end{aligned}$$

With virtual control variables (25) and (26),

$$\dot{\mathcal{V}}_\gamma(h - h_{\rm re}, e_\gamma) = (h - h_{\rm re})V\sin\gamma_{\rm re} - k_\gamma(\gamma - \gamma_{\rm re})^2 \leq 0,$$

$$\dot{\mathcal{V}}_q(\alpha - \alpha_{\rm re}, e_q) = -k_\alpha(\alpha - \alpha_{\rm re})^2 - k_q(q - q_{\rm re})^2 \leq 0.$$

That means h, γ and α, q are all stabilized according to Lyapunov theory. Further introduce (25) into above $q_{\rm re}$, and (28) is obtained.

In general, the stabilization of nominal quad-TRUAV model is ensured by backstepping, and a hierarchical nonlinear controller is formulated for reference tracking.